Desalination and Water Treatment
www.deswater.com
doi: 10.1080/19443994.2015.1102089

57 (2016) 18630–18638
August

Taylor & Francis
Taylor & Francis Group

Modeling and optimization of treatment of milk industry wastewater using chitosan–zinc oxide nanocomposite

K. Thirugnanasambandham, V. Sivakumar*

Department of Chemical Engineering, AC Tech Campus, Anna University, Chennai 600025, Tamil Nadu, India, emails: thirusambath5@gmail.com (K. Thirugnanasambandham), drvsivakumar@yahoo.com (V. Sivakumar)

Received 11 March 2015; Accepted 10 September 2015

ABSTRACT

The main objective of the present study was to investigate and optimize the operating parameters in synthesis of chitosan–zinc oxide nanocomposite (CZO) composite beads for the application in milk processing industry wastewater. The resulting nanocomposite was characterized by infrared spectroscopy (FT-IR). Individual and interactive effects of process parameters were studied using response surface methodology coupled with Box–Behnken design. The results showed that the optimized conditions were initial pH of 4.92, CZO composite dose of 1.5 g/L, contact time of 45 min, and amount of dilution of 12%. Under these conditions, 89% of turbidity and 97% of chemical oxygen demand were reduced.

Keywords: Milk industry wastewater; Chitosan; Zinc oxide; Box–Behnken design; Optimization

1. Introduction

Water is the essential material for all life on earth and a valuable source for human civilization [1]. Reliable access to clean and affordable water is considered one of the most basic humanitarian goals, and remains a major global challenge for the twenty-first century [2]. Ever increasing industrialization and rapid population growth have considerably increased the rate of water pollution worldwide [3]. The pollution of water resources due to discharge of poor quality effluents poses a serious threat to human beings and aquatic organisms since they rely on water for sustenance [4]. The problem is more severe in developing countries like India where rapid population growth and industrialization [5]. Among various kinds of industries in India, milk processing industry is of crucial importance [6]. The milk processing industries require large quantity of fresh water from natural water resources like rivers for the purpose of washing of cans, machinery, and floor. The clean water is used in various stages of milk processing operations such as milk processing, cleaning, packaging, and cleaning of the milk tankers. Moreover, fresh water is used for processing in the ratio of 1:10 (water:milk) per liter of milk [7]. Milk processing industry wastewater has high concentration of dissolved organic components like whey proteins, lactose, fat, and minerals, and it is also malodorous because of the decomposition of some of the contaminants causing discomfort to the surrounding population [8]. The milk processing industry generates huge amount of wastewaters, approximately 0.4–20 L of waste per liter of processed milk [9]. Discharge of milk processing industry wastewater with high levels of chemical oxygen demand (COD), biochemical oxygen demand (BOD), oil and grease, nitrogen, and phosphorus into nearby water bodies causes

*Corresponding author.

the negative impact. Hence, there is a critical need to develop an effective milk processing industry wastewater treatment method, prior to its disposal into ecological system.

Last few decades, applications of nanotechnology for the remediation of contaminated industrial wastewater using nanoparticles is one of the most prominent technology with considerable potential benefits [10]. It has been postulated that nanoparticles incorporated polymers can remove turbidity, COD from industrial wastewaters. Chitosan is the alkaline deacetylated product of chitin, which is derived from the exoskeleton of crustaceans [11]. It is nontoxic, hydrophilic, biocompatible, biodegradable, and antibacterial polymer. Chitosan and its derivatives have great potential applications in the areas of biotechnology, biomedicine, food ingredients, and cosmetics. Noteworthily, chitosan is also capable of removing a COD and BOD, because its amino groups can serve as chelation sites [12]. Thus, the binding of chitosan onto zinc oxide nanoparticles will probably yield another novel nano-adsorbent for the efficient removal of COD and BOD from industrial wastewaters. There are, however, many uncertainties regarding the fundamental features of this technology, which have made it difficult to engineer applications for optimal performance. This important aspect of nano-adsorbents needs extensive considerations as well [13].

Hence, in the present study effort has been made to prepare the chitosan–zinc oxide nanoparticles (CZO) composite beads and investigate its efficiency to treat milk processing industry wastewater. The prepared chitosan–ZnO nanocomposites were investigated by infrared spectroscopy (FT-IR). Individual and interactive effect of process variables such as initial pH, CZO composite dose, contact time, and amount of dilution on the percentage removal of turbidity and COD were analyzed using four factors three levels Box–Behnken response surface design (BBD). The outcome of the study will create the novel opportunity to know the in-depth knowledge of mechanism behind CZO composite beads application to treat milk processing industry wastewater.

2. Materials and methods

2.1. Raw wastewater and chemicals

The wastewater used in this study was collected from Erode, Tamil Nadu, India and it was stored at 4℃ prior to the experiments. The characteristics of wastewater are determined and it is found to be: initial pH of 6.5, turbidity of 1,524 NTU, and COD of 7,640 mg/L. Chitosan was purchased from Sigma Chemicals, Chennai. Zinc Oxide was purchased from Merck Chemicals, Mumbai. All the chemicals (HCl and NaOH) used in this study were of anlaytical grade and purchased from local suppliers from Erode, Tamil Nadu.

2.2. Preparation of CZO composite beads

A 0.75 g of zinc oxide (Zno) powder was dissolved in 100 ml of 1% acetic acid by adding 10 ml of 60% HNO_3 (nitric acid). Then, 1 g of chitosan was added to this solution. After that, sonication process was performed for 15 min and pH of the solution is increased up to 10 by adding drop by drop NaOH solution. The solution was kept in water bath at 60℃ for about 3 h. The mixture was filtered and washed with deionized water and then it was dried in an oven at 50℃ for 1 h. The preparation procedure employed has been reported elsewhere with some modification [14].

2.3. Characterization of CZO composites

Fourier transform infrared spectroscopy (FT-IR) of nanocomposite samples was recorded on FTIR spectrometer using KBr powder as a reference.

2.4. Analytical methods

The removal efficiency (RE) of turbidity and COD are calculated using the following equation [15]:

$$\mathrm{RE} = \left(\frac{c_0 - c_e}{c_0}\right) \times 100 \quad (1)$$

where c_0 and c_e are the initial and final concentrations of turbidity and COD, respectively.

2.5. Statistical experimental design

In this present study, four factors three level Box–Behnken response surface experimental design (BBD) was applied to investigate the individual and interactive effects of process variables including initial pH, CZO composite dose, contact time, and amount of dilution on the percentage removal of turbidity , COD removal from milk processing industry wastewater. The independent variables and their levels are presented in Table 1. Twenty-nine batch experiments were designed with five replications using the following equation (Table 2). The correlation between the responses and independent variables were evaluated by developing the second-order polynomial

Table 1
Ranges of independent variables and their levels

Variables (unit)	Factors X	Level −1	0	1
Initial pH	A	2	5	8
CZO composite dose (g/L)	B	0.5	1.25	2
Contact time (min)	C	20	60	100
Amount of dilution (%)	D	10	25	40

mathematical models. The generalized form of equation was given below [16]:

$$Y = \beta_0 + \sum_{j=1}^{k} \beta_j X_j + \sum_{j=1}^{k} \beta_{jj} X_j^2 + \sum_{i} \sum_{<j=2}^{k} \beta_{ij} X_i X_j + e_i \quad (2)$$

where Y is the response; X_i and X_j are variables (i and j range from 1 to k); β_0 is the model intercept coefficient; β_j, β_{jj} and β_{ij} are interaction coefficients of linear, quadratic, and the second-order terms, respectively; k is the number of independent parameters and e_i is the error. Adequacy of the developed mathematical models was examined using predicted vs. actual plots and analysis of variance (ANOVA). Three-dimensional (3D) response surface contour graphs were plotted from developed mathematical models in order to study the interactive effect of independent variables on the responses. Finally, numerical optimization coupled with Derringer's desired function methodology was employed to optimize the process variables. Design-Expert 8.0.7.1 (State-Ease Inc., Minneapolis, MN, USA) statistical package was employed for all the statistical calculations [17].

3. Results and discussions

3.1. Chracterization of CZO composite beads

The FT-IR spectra of chitosan and CZO are shown in Fig. 1(a). The FT-IR spectra of pure chitosan (a spectrum) show bands at 3,409 cm^{-1} due to the stretching

Table 2
BBD and their experimental results

Run	A	B	C	D	Turbidity removal (%)	COD removal (%)
1	8	2	60	25	44.55	48.65
2	2	2	60	25	35.47	42.56
3	5	2	60	10	65.45	71.05
4	2	1.25	100	25	44.45	50.28
5	5	1.25	60	25	87.54	89.57
6	5	2	60	40	49.45	53.17
7	5	1.25	60	25	88.54	87.69
8	5	1.25	20	40	59.25	63.27
9	5	0.5	100	25	77.53	80.87
10	2	0.5	60	25	19.45	23.27
11	5	2	20	25	87.53	84.21
12	5	0.5	60	40	54.55	58.53
13	5	2	100	25	32.41	39.19
14	5	1.25	60	25	88.54	89.57
15	8	0.5	60	25	54.45	57.27
16	5	1.25	100	40	58.55	62.17
17	8	1.25	60	40	50.55	55.48
18	8	1.25	20	25	65.45	72.48
19	8	1.25	100	25	25.87	32.85
20	5	0.5	20	25	33.75	34.58
21	5	1.25	20	10	73.85	77.47
22	5	1.25	60	25	88.54	89.57
23	2	1.25	20	25	27.81	38.99
24	5	0.5	60	10	61.54	63.19
25	8	1.25	60	10	58.95	68.15
26	5	1.25	100	10	78.13	83.29
27	2	1.25	60	10	58.64	62.54
28	2	1.25	60	40	25.47	31.54
29	5	1.25	60	25	88.54	89.57

vibration mode of OH and NH_2 groups. The peaks at 2,933 and 2,868 cm^{-1} are typical of CAH stretching vibration, while the band at 1,651 cm^{-1} is due to the amide I group (CAO stretching along with NAH deformation mode), 1,612 cm^{-1} peak is attributed to the NH_2 group due to NAH deformation, 1,415 cm^{-1} peak is due to CAN axial deformation (amine group band), 1,382 cm^{-1} peak is due to the COOA group in carboxylic acid salt, 1,162 cm^{-1} is assigned to the special broad peak of b glucosidic band in polysaccharide unit, 1,042 cm^{-1} is attributed to the stretching vibration mode of the hydroxyl group, 1,027 cm^{-1} stretching vibration of CAOAC in glucose circle and 1,080–1,020 cm^{-1} bands correspond to CHAOH in cyclic compounds. In comparison with chitosan, the broader and stronger peak shifted considerably to lower wavenumber at 3,366 cm^{-1}, which indicates strong attachment of ZnO to the amide groups of chitosan molecules. The absorption peaks at 2,914, 2,878 cm^{-1} are due to asymmetric stretching of CH_3 and CH_2 of chitosan polymer. The absorption peaks at 1,656 and 1,073 cm^{-1} are attributed to bending vibration of the ANH_2 group and the CAO stretching group. A new broad absorption band at the range of 580–400 cm^{-1} was found in the FT-IR spectra of CZO nanocomposite, which were ascribed to the vibration of OAZnAO groups. The reason for the above phenomena was the formation of hydrogen bonds between ZnO and chitosan. This result indicated that the CZOs composite has been prepared successfully without damaging the crystal structure of ZnO core [18,19].

3.2. Development of mathematical model

Recently, response surface methodology (RSM) has been applied in wide range of processes, such as absorption [19], biodiesel production [20]; biological wastewater treatment [21]; biosorption [22], engine performance [23] and others. Removal of turbidity and COD from milk processing industry wastewater using CZO nanocomposite beads are investigated under various process variables such as initial pH, CZO composite dose, contact time, and amount of dilution using RSM. Different response functions such as linear, interactive, quadratic, and cubic models are employed to compare the experimental data (Table 2). In order to find out the effective mathematical model, two different tests namely sequential model sum of squares and model summary statistics were carried out on the BBD and the results are presented in Tables 3 and 4. Sequential model sum of squares and model summary statistics showed that the second-order polynomial model provided the best fit to experimental data with the highest correlation coefficient (R^2), adjusted R^2, predicted R^2 values, and the higher F-value and lowest p-value. Therefore, the second-order polynomial model is selected for the further analysis. The developed second-order polynomial model is as follows [24]:

$$Y_1 = 88.34 + 7.38A + 1.13B - 2.56C - 8.23D - 6.48AB - 14.06AC + 6.19AD - 24.73BC - 2.25BD - 1.24CD - 32.08A^2 - 18.95B^2 - 12.89C^2 - 9.17D^2 \quad (3)$$

$$Y_2 = 89.19 + 7.14A + 1.76B - 1.87C - 8.46D - 6.98AB - 12.74AC + 4.58AD - 22.83BC - 3.30BD - 1.73CD - 28.05A^2 - 18.99B^2 - 11.11C^2 - 7.32D^2 \quad (4)$$

where A, B, C, and D are initial pH, CZO composite dose, contact time, and amount of dilution, respectively.

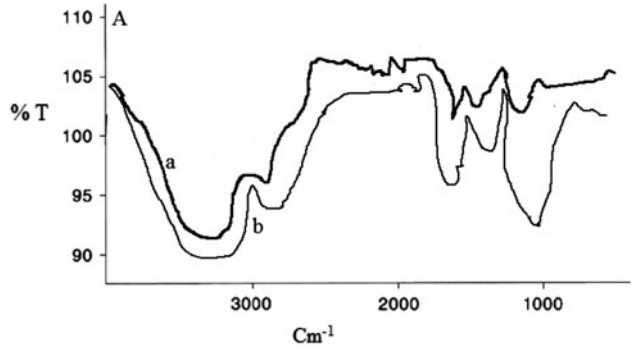

Fig. 1. FT-IR spectra of nanocomposite.

3.3. Adequacy of developed mathematical model

ANOVA results for the second-order polynomial regression models are shown in Table 5. The prob. > F-values found for the models were <0.05, which indicated that the model terms were significant at a probability level of 95% [25]. The ANOVA result for the responses of Y_1 and Y_2, showed F-values greater than 10, which implied that the terms in the models have significant effects on the responses. The large F-value indicates that most of the variation in the response can be explained by the regression equation. The models provided higher correlation coefficients (R^2) and adjusted correlation coefficients (adj-R^2) for Y_1

Table 3
Sequential model sum of squares for responses

Source	Sum of squares	DF	Mean square	*F*-value	Prob. > *F*	Remarks
Sequential model sum of squares for turbidity removal						
Mean	97,881	1	97,881			
Linear	1,560	4	390	0.79	0.5428	
2FI	3,583	6	597	1.30	0.3058	
Quadratic	7,949	4	1987	91.46	<0.0001	Suggested
Cubic	230	8	29	2.32	0.1608	Aliased
Residual	74	6	12			
Total	111,277	29	3,837			
Sequential model sum of squares for COD removal						
Mean	111,845	1	111,845			
Linear	1,549	4	387	0.94	0.4561	
2FI	3,068	6	511	1.36	0.2845	
Quadratic	6,458	4	1,614	68.46	<0.0001	Suggested
Cubic	304	8	38	8.64	0.0085	Aliased
Residual	26	6	4			
Total	123,250	29	4,250			

Table 4
Model summary statistics for responses

Source	Std. dev.	R^2	Adjusted R^2	Predicted R^2	PRESS	Remarks
Model summary statistics for turbidity removal						
Linear	22.2077	0.1164	−0.0308	−0.2158	16,286.6279	
2FI	21.4127	0.3839	0.0416	−0.2780	17,119.4264	
Quadratic	4.6612	0.9773	0.9546	0.8695	1,748.7225	Suggested
Cubic	3.5205	0.9944	0.9741	0.2091	10,594.2584	Aliased
Model summary statistics for COD removal						
Linear	20.2650	0.1358	−0.0082	−0.1950	13,629.1052	
2FI	19.4191	0.4049	0.0742	−0.2521	14,280.9792	
Quadratic	4.8563	0.9711	0.9421	0.8343	1,889.8828	Suggested
Cubic	2.0964	0.9977	0.9892	0.7024	3,394.5896	Aliased

and Y_2, respectively, which were high and demonstrate a significant and intense correlation between the observed and predicted values [26]. The adequate precision values of the models compare the predicted data at the design points with the average prediction error. In the present study, adequate precision values were obtained as >4, indicating an appropriate signal, and suggested that the regression models could be used to navigate the design space [27]. The obtained CV% values also confirmed the adequacy of the developed models. In order to validate the adequacies of developed mathematical models, experimental values were selected randomly from selected process variable ranges and are plotted with model predicted vs. (Fig. 2). This plot help us to find out the relationship between predicted and experimental values and the data points on this plot lie very close to the diagonal line, which indicates the good adequate agreement between experimental data. From these results, it is concluded that the developed mathematical models can describe the present experimental design [21]. Generally, all response surfaces (Figs. 3–5) were convex in nature, suggesting that there was a well-defined optimum point for maximum turbidity and COD removals.

3.4. Effect of process variables on treatment effciency

The relationship between independent and dependent variables are illustrated by the representation of 3D response surface contours plots generated from the developed mathematical models and are shown in Figs. 3–5. In this study, the model has more than two factors. So, the response surface contour plots are

Table 5
ANOVA table for responses

Source	Turbidity removal (%)		COD removal (%)	
	F-value	*p*-value	*F*-value	*p*-value
Model	43.04	<0.0001	33.54	<0.0001
A	30.06	<0.0001	25.92	0.0002
B	0.71	0.4141	1.58	0.2299
C	3.61	0.0780	1.77	0.2043
D	37.39	<0.0001	36.43	<0.0001
AB	7.73	0.0147	8.26	0.0123
AC	36.37	<0.0001	27.54	0.0001
AD	7.06	0.0188	3.56	0.0800
BC	112.55	<0.0001	88.38	<0.0001
BD	0.93	0.3502	1.85	0.1950
CD	0.29	0.6016	0.51	0.4879
A^2	307.18	<0.0001	216.47	<0.0001
B^2	107.20	<0.0001	99.16	<0.0001
C^2	49.63	<0.0001	33.92	<0.0001
D^2	25.09	0.0002	14.75	0.0018
C.V. %	8.02		7.82	
AP	19.58		18.01	

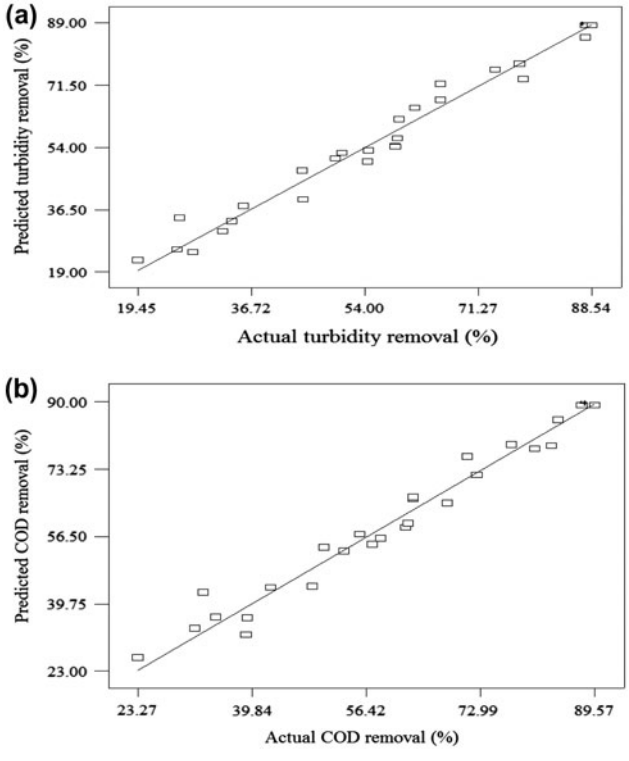

Fig. 2. Predicted vs. actual plot for responses: (a) turbidity and (b) COD.

drawn by maintaining one factor at a constant level (in turn at its central level), whereas the other two factors were varied in their range.

3.4.1. Effect of initial pH

The influence of pH on the treatment of milk processing industry wastewater using CZOs composite is shown in Fig. 3. The results indicated that the removal percentage of turbidity and COD increased with increasing pH up to 7, and then decreased. The effect of pH can be explained by interaction between the composite surface and the sorbate. At different pH values, the functional groups of chitosan may be dissociated as their dissociation constants, and therefore, could take part in the surface complexation. In basic media, the decrease in the amount of turbidity and COD removal is due to the phenomenon of partial dissolution [28].

3.4.2. Effect of CZO composite dose

Effect of CZO composite dose on turbidity and COD removal percentage is investigated using CZO composite. The experiments were performed by different concentrations of CZO composite, which showed that the RE increased with an increase in CZO composite up to 1.5 g/L (Fig. 3). After a very slow increase in removal percentage, it is found that the increase in CZO composite dose of more than 1.5 g/L dose did not affect the removal percentage significantly. This may be presumed that the availability of active sites on the nanocomposite is decreasing at higher doses of sorbents (>1.5 g/L). The total active surface area increases by increasing composite dosage. Beyond the CZO composite dose of 1.5 g/L shows the negligible amount of removal efficiencies [29].

3.4.3. Effect of contact time

The influence of contact time (20–100 min) on CZO nanocomposite are monitored. Fig. 4 shows the effect of contact time on the treatment of milk processing industry wastewater using CZO nanocomposite. The plot shows that the removal of turbidity and COD increased with increasing contact time and then decreases a value beyond which no more turbidity and COD would be further removed from the milk processing industry wastewater. The initial fast rate is probably due to the abundant available binding sites on the surface of the adsorbent. After that, other vacant surface sites were difficult to be absorbed due to repulsive forces between the adsorbate molecules on the adsorbent, hence RE is decreased.

3.4.4. Effect of amount of dilution

The influence of amount of dilution of turbidity and COD over a range of 10–40% is illustrated in Fig. 4. From the results, the removal percentage of turbidity and COD decreased by decrease in amount of dilution. When the dilution increases, less organic substances are adsorbed on the surface of the sorbent, thus, the removal efficiencies are decreased. Perturbation plot is shown in Fig. 5, which is also in close agreement with Figs. 3 and 4.

3.5. Optimization

Numerical optimization technique coupled with Derringer's desired function methodology is employed to optimize the process parameters to treat milk processing industry wastewater using CZO composite. The results showed that the optimized conditions were initial pH of 4.92, CZO composite dose of 1.52 g/L, contact time of 44.85 min, and amount of dilution of 12.12%. Under these conditions, 89.23% of turbidity and 97.11% of COD were reduced. However, considering the operability in actual treatment process, the optimal conditions can be modified as follows: initial pH of 5, CZO composite dose of 1.5 g/L, contact time of 45 min and amount of dilution of 12%.

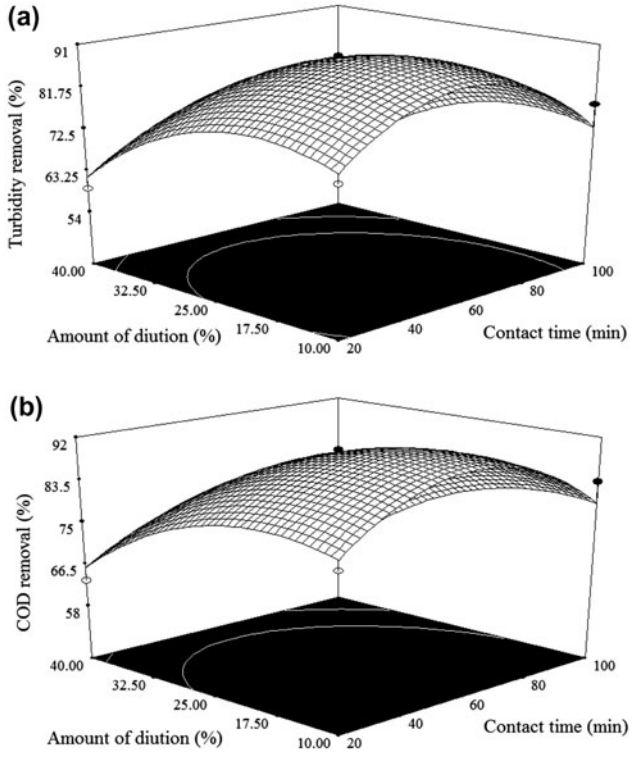

Fig. 4. Effect of contact time and amount of dilution on responses: (a) turbidity and (b) COD.

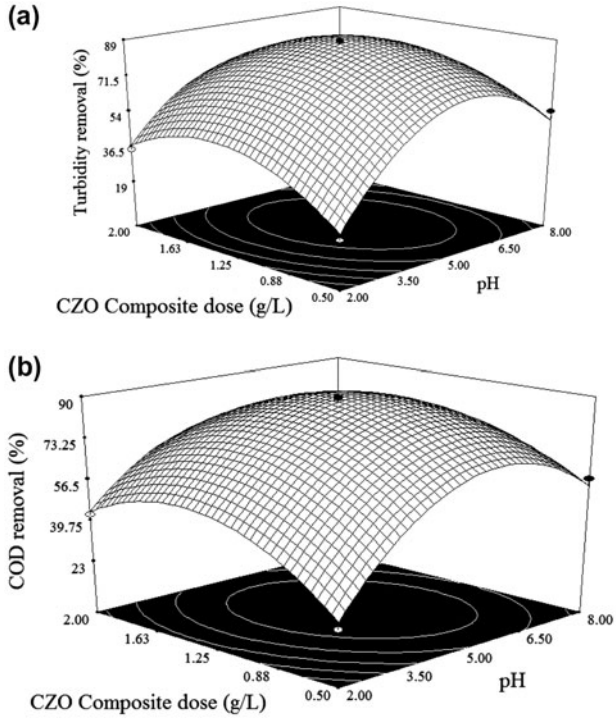

Fig. 3. Effect of initial pH and CZO composite dose on responses: (a) turbidity and (b) COD.

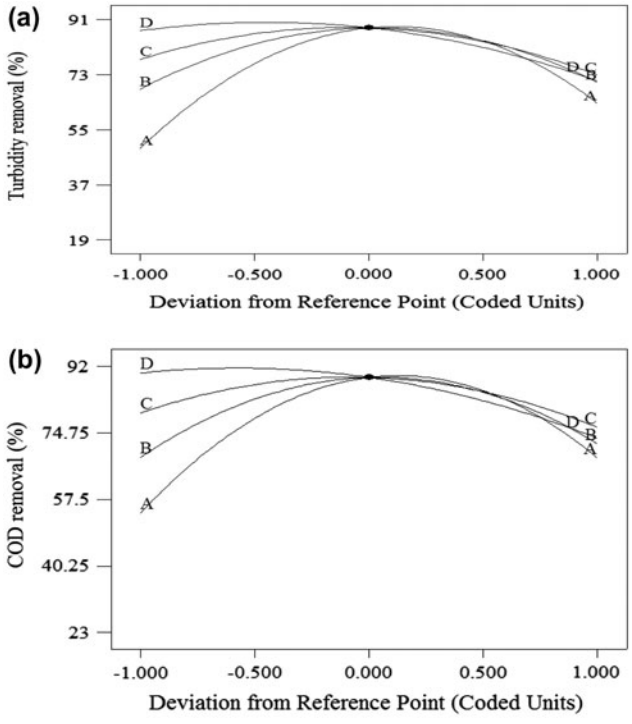

Fig. 5. Perturbation plot for milk processing industry wastewater treatment process: (a) turbidity and (b) COD.

Table 6
Study results (COD and turbidity removals) as compared to using other adsorption process in treatment of milk or dairy industry wastewater

S. No.	Adsorption process	Present study
COD	81	97
Turbidity	78	89

Under these conditions, 89% of turbidity and 97% of COD were reduced, which are in close agreement with the predicted values. Table 6 shows the present study results (COD and turbidity removals) as compared to using other adsorption process in treatment of milk industry wastewater. From the results, it is found that the present method is suitable to treat milk industry wastewater.

4. Conclusions

RSM coupled with four factors three level Box–Behnken response surface experimental design (BBD) was employed to optimize the process variables in the treatment of milk processing industry wastewater using chitosan–zinc oxide nanocomposite. Second-order polynomial mathematical models were developed with good coefficient of determination values ($R^2 > 0.95$) for turbidity removal and COD removal. ANOVA showed the significant effect of each process variables on the treatment efficiency. Optimum operating conditions were determined using numerical optimization method and it is found to be; initial pH of 5, CZO composite dose of 1.5 g/L, contact time of 45 min, and amount of dilution of 12%. Under these conditions, 89% of turbidity and 97% of COD were reduced.

References

[1] G.C. Cordeiro, R.D. Toledo-Filho, L.M. Tavares, E.M.R. Fairbairn, Ultrafine grinding of sugar cane bagasse ash for application as pozzolanic admixture in concrete, Cem. Concr. Res. 39 (2009) 110–115.
[2] J. Prakash Maran, S. Manikandan, K. Thirugnanasambandham, C. Vigna Nivetha, R. Dinesh, Box–Behnken design based statistical modeling for ultrasound-assisted extraction of corn silk polysaccharide, Carbohydr. Polym. 92 (2013) 604–611.
[3] C. Wang, W. Chou, M. Chung, Y. Kuo, COD removal from real dyeing wastewater by electro-Fenton technology using an activated carbon fiber cathode, Desalination 253 (2010) 129–134.
[4] J. Maran, V. Sivakumar, R. Sridhar, K. Thirugnanasambandham, Development of model for barrier and optical properties of tapioca starch based edible films Carbohydr. Polym. 92 (2013) 1335–1347.
[5] J. Feng, Y. Sun, Z. Zheng, J. Zhang, S. Li, Y. Tian, Treatment of tannery wastewater by electrocoagulation, J. Environ. Sci. 19 (2007) 1409–1415.
[6] O. Lefebvre, N. Vasudevan, M. Torrijos, Halophilic biological treatment of tannery soak liquor in a sequencing batch reactor, Water Res. 39 (2005) 1471–1480.
[7] G. Lofrano, S. Meric, M. Inglese, A.D. Nikolau, V. Belgiorno, Fenton oxidation treatment of tannery wastewater and tanning agents: Synthetic tannin and nonylphenol ethoxylate based degreasing agent, Desalin. Water Treat. 23 (2010) 173–180.
[8] L. D'antonio, R.M.A. Napoli, Dewaterability of MBR sludge loaded with tannery wastewater, Desalin. Water Treat. 23 (2010) 129−134.
[9] K. Ganesan, K. Rajagopal, K. Thangavel, Evaluation of bagasse ash as supplementary cementitious material, Cem. Concr. Compos. 29 (2007) 515–524.
[10] J.H. Jhamandas, M.B. Wie, K. Harris, D. MacTavish, S. Kar, Eur. J. Neurosci. 21 (2005) 2649–2659.
[11] K. Thirugnanasambandham, V. Sivakumar, J. Prakash maran, Optimization of electrocoagulation process to treat biologically pretreated bagasse effluent, J. Serb. Chem. Soc. 79 (2013) 74–74.
[12] K. Thirugnanasambandham, V. Sivakumar, J. Prakash Maran, Treatment of egg processing industry effluent using chitosan as an adsorbent, J. Serb. Chem. Soc. 79(6) (2014) 743–757.
[13] J.F. Martirena Hernández, B. Middendorf, M. Gehrke, H. Budelmann, Use of wastes of the sugar industry as pozzolana in lime-pozzolana binders: Study of the reaction, Cem. Concr. Res. 28 (1998) 1525–1536.
[14] S. Bayar, Y. Yıldız, A. Yılmaz, Ş. İrdemez, The effect of stirring speed and current density on removal efficiency of poultry slaughterhouse wastewater by electrocoagulation method, Desalination 280 (2011) 103–107.
[15] G.C. Cordeiro, R.D. Toledo-Filho, E.M.R. Fairbairn, Effect of calcination temperature on the pozzolanic activity of sugar cane bagasse ash, Constr. Build. Mater. 23 (2009) 3301–3303.
[16] J. Zhong, X. Zhang, Y. Ren, J. Yang, H. Tan, J. Zhou, Optimization of *Bacillus subtilis* cell growth effecting jiean-peptide production in fed batch fermentation using central composite design, Electron. J. Biotechnol. 17 (2014) 132–136.
[17] K. Thirugananasambandham, V. Sivakumar, J. Prakash Maran, S. Kandasamy, Treatment of rice mill wastewater using continuous electrocoagulation technique: optimization and modelling, J. Korean Chem. Soc. 57 2013 761–768.
[18] K. Thirugnanasambandham, V. Sivakumar, J. Prakash Maran J, Bagasse wastewater treatment using biopolymer—A novel approach, J. Serb. Chem. Soc. 79(7) (2014) 897–909.
[19] A.D. Bhanarkar, R.K. Gupta, R.B. Biniwale, S.M. Tamhane, Nitric oxide absorption by hydrogen peroxide in airlift reactor: A study using response surface methodology, Int. J. Environ. Sci. Technol. 11 (2014) 1537–1548.
[20] G. Moradi, F. Mohammadi, Utilization of waste coral for biodiesel production via transesterification of soybean oil, Int. J. Environ. Sci. Technol. 11 (2014) 805–812.

[21] N. Kornochalert, D. Kantachote, S. Chaiprapat, S. Techkarnjanaruk, Bioaugmentation of latex rubber sheet wastewater treatment with stimulated indigenous purple nonsulfur bacteria by fermented pineapple extract, Electron. J. Biotechnol. 17 (2014) 174–182.
[22] P. Aytar, S. Gedikli, Y. Buruk, A. Cabuk, N. Burnak, Lead and nickel biosorption with a fungal biomass isolated from metal mine drainage: Box–Behnken experimental design, Int. J. Environ. Sci. Technol. 11 (2014) 1631–1640.
[23] K. Sivaramakrishnan, P. Ravikumar, Optimization of operational parameters on performance and emissions of a diesel engine using biodiesel, Int. J. Environ. Sci. Technol. 11 (2014) 949–958.
[24] M.S. Secula, I. Cretescu, B. Cagnon, L.R. Manea, C.S. Stan, I.G. Breaban, Fractional factorial design study on the performance of GAC-enhanced electrocoagulation process involved in color removal from dye solutions, Materials 6 (2013) 2723–2746.
[25] B. Brzozowski, M. Lewandowska, M. Prolyl, Prolyl endopeptidase—Optimization of medium and culture conditions for enhanced production by Lactobacillus acidophilus, Electron. J. Biotechnol. 17 (2014) 204–210.
[26] W. Subramonian, T.Y. Wu, S.P. Chai, An application of response surface methodology for optimizing coagulation process of raw industrial effluent using *Cassia obtusifolia* seed gum together with alum, Ind. Crops Prod. 70 (2015) 107–115.
[27] H.T. Tan, G.A. Dykes, T.Y. Wu, L.F. Siow, Enhanced xylose recovery from oil palm empty fruit bunch by efficient acid hydrolysis, Appl. Biochem. Biotechnol. 170 (2013) 1602–1613.
[28] C.Y. Teh, T.Y. Wu, J.C. Juan, Optimization of agro-industrial wastewater treatment using unmodified rice starch as a natural coagulant, Ind. Crops Prod. 56 (2014) 17–26.
[29] T.Y. Wu, A.W. Mohammad, J.M. Jahim, N. Anuar, Optimized reuse and bioconversion from retentate of pre-filtered palm oil mill effluent (POME) into microbial protease by *Aspergillus terreus* using response surface methodology, J. Chem. Technol. Biotechnol. 84 (2009) 1390–1396.